DOI:
10.1038/s41562-019-0738-8

Document Version
Peer reviewed version

Identification of neurobehavioural symptom groups based on shared brain mechanisms

Authors: Alex Ing, Ph.D.[1]; Philipp G. Sämann, M.D.[2], Ph.D.; Congying Chu, Ph.D.[1]; Nicole Tay, Ph.D.[1]; Francesca Biondo, Ph.D.[1]; Gabriel Robert, M.D.[1,3]; Tianye Jia, Ph.D.[1]; Thomas Wolfers[4]; Sylvane Desrivières Ph.D.[1]; Tobias Banaschewski M.D.; Ph.D.[5]; Arun L.W. Bokde Ph.D.[6]; Uli Bromberg Ph.D.[7]; Christian Büchel M.D.[7,8]; Patricia Conrod[9,10]; Tahmine Fadai[7]; Herta Flor Ph.D.[11,12]; Vincent Frouin Ph.D.[13]; Hugh Garavan Ph.D.[14]; Philip A. Spechler, M.A[14]; Penny Gowland Ph.D.[15]; Yvonne Grimmer[5]; Andreas Heinz M.D., Ph.D.[16]; Bernd Ittermann Ph.D.[17]; Viola Kappel[18]; Jean-Luc Martinot M.D., Ph.D.[19]; Andreas Meyer-Lindenberg M.D., Ph.D.[20]; Sabina Millenet Dipl.-Psych.[5]; Frauke Nees Ph.D.[5,11]; Betteke van Noort[18]; Dimitri Papadopoulos Orfanos Ph.D.[13]; Marie-Laure Paillère Martinot[21]; Jani Penttilä[22]; Luise Poustka M.D.[23]; Erin Burke Quinlan Ph.D.[1]; Michael N. Smolka M.D.[24]; Argyris Stringaris[25,26]; Maren Struve[24]; Ilya M. Veer Ph.D.[16]; Henrik Walter M.D., Ph.D[16]; Robert Whelan Ph.D.[27]; Ole A. Andreassen, M.D., Ph.D.[28,29]; Ingrid Agartz, M.D., Ph.D.[29,30,31]; Hervé Lemaitre[32]; Edward D. Barker[33,1]; John Ashburner, Ph.D.[34], Elisabeth Binder M.D.[2], Ph.D.; Jan Buitelaar M.D., Ph.D.[4] ; Andre Marquand Ph.D.[4]; Trevor W. Robbins, Ph.D.[35], Gunter Schumann M.D., Ph.D.[1,36]*; IMAGEN Consortium.

Affiliations:

[1] Centre for Population Neuroscience and Precision Medicine (PONS), Institute of Psychiatry, Psychology & Neuroscience, SGDP Centre, King's College London, London, United Kingdom;

[2] Neuroimaging, Max Planck Institute of Psychiatry, Munich, Germany;

[3] Behavior and Basal Ganglia research unit, University of Rennes, Rennes, France;

[4] Donders Institute for Brain, Cognition and Behaviour, Radboud University, Nijmegen, The Netherlands;

[5] Department of Child and Adolescent Psychiatry and Psychotherapy, Central Institute of Mental Health, Medical Faculty Mannheim, Heidelberg University, Mannheim, Germany;

[6] Discipline of Psychiatry, School of Medicine and Trinity College Institute of Neuroscience, Trinity College Dublin, Dublin, Ireland;

[7] Systems Neuroscience, University Medical Centre Hamburg-Eppendorf, Hamburg, Germany;

[8] Department of Psychology, Stanford University, Stanford, California USA;

[9] Department of Psychological Medicine, Institute of Psychiatry, Psychology & Neuroscience, King's College London, UK;

[10] Department of Psychiatry, Université de Montréal, CHU Ste Justine Hospital, Montreal QC, Canada;

[11] Institute of Cognitive and Clinical Neuroscience, Central Institute of Mental Health, Medical Faculty Mannheim, Heidelberg University, Mannheim, Germany;

[12] Department of Psychology, School of Social Sciences, University of Mannheim, Mannheim, Germany;

[13] NeuroSpin, CEA, Université Paris-Saclay, Gif-sur-Yvette, France;

[14] Departments of Psychiatry and Psychology, University of Vermont, Burlington, Vermont, USA;

[15] Sir Peter Mansfield Imaging Centre School of Physics and Astronomy, University of Nottingham, University Park, Nottingham, United Kingdom;

[16] Department of Psychiatry and Psychotherapy CCM, Charité – Universitätsmedizin Berlin, corporate member of Freie Universität Berlin, Humboldt-Universität zu Berlin, and Berlin Institute of Health, Berlin, Germany;

[17] Biomedical Magnetic Resonance**,** Physikalisch-Technische Bundesanstalt (PTB), Braunschweig and Berlin, Germany;

[18] Department of Child and Adolescent Psychiatry Psychosomatics and Psychotherapy, Charité, Humboldt University, Berlin, Germany;

[19] Institut National de la Santé et de la Recherche Médicale, INSERM Unit 1000 "Neuroimaging & Psychiatry", University Paris Saclay, University Paris Descartes; DIgiteo-Labs, Gif-sur-Yvette; and Maison de Solenn, Paris, France;

[20] Department of Psychiatry and Psychotherapy, Central Institute of Mental Health, Medical Faculty Mannheim, Heidelberg University, Mannheim, Germany;

[21] Institut National de la Santé et de la Recherche Médicale, INSERM Unit 1000 "Neuroimaging & Psychiatry", University Paris Saclay, University Paris Descartes; DIgiteo-Labs, Gif-sur-Yvette; and AP-HP.Sorbonne Université, Department of Child and Adolescent Psychiatry, Pitié-Salpêtrière Hospital, Paris, France;

[22] Department of Social and Health Care, Psychosocial Services Adolescent Outpatient Clinic, Lahti, Finland;

[23] Department of Child and Adolescent Psychiatry and Psychotherapy, University Medical Centre Göttingen, Göttingen, Germany;

[24] Department of Psychiatry and Neuroimaging Center, Technische Universität, Dresden, Dresden, Germany;

[25] Department of Child and Adolescent Psychiatry, Institute of Psychiatry, Psychology & Neuroscience, King's College London, London, United Kingdom;

[26] Mood Brain and Development Unit (MBDU), National Institute of Mental Health / NIH, Bethesda MD, USA;

[27] School of Psychology and Global Brain Health Institute, Trinity College Dublin, Dublin, Ireland;

[28] Division of Mental Health and Addiction, Oslo University Hospital, Oslo, Norway;

[29] NORMENT, Institute of Clinical Medicine, University of Oslo, Oslo, Norway;

[30] Department of Psychiatric Research, Diakonhjemmet Hospital, Oslo, Norway;

[31] Department of Clinical Neuroscience, Centre for Psychiatric Research, Karolinska Institutet, Stockholm, Sweden;

[32] Institut National de la Santé et de la Recherche Médicale, UMR 992 INSERM, CEA, Faculté de médecine, Université Paris-Sud, Université Paris-Saclay, NeuroSpin, Gif-sur-Yvette, France;

[33] Department of Psychology, Institute of Psychiatry, Psychology and Neuroscience, King's College London, London, United Kingdom;

[34] Wellcome Centre for Human Neuroimaging, UCL Institute of Neurology, University College London, London, United Kingdom;

[35] Department of Psychology and Behavioural and Clinical Neuroscience Institute, University of Cambridge, Cambridge, United Kingdom;

[36] PONS Research Group, Dept of Psychiatry and Psychotherapy, Campus Charite Mitte, Humboldt University, Berlin and Leibniz Institute for Neurobiology, Magdeburg, Germany, and Institute for Science and Technology of Brain-inspired Intelligence (ISTBI), Fudan University, Shanghai, P.R. China.

Abstract:

Most psychopathological disorders develop in adolescence. The biological basis for this development is poorly understood. To enhance diagnostic characterisation, and develop improved targeted interventions, it is critical to identify behavioural symptom groups that share neural substrates. We ran analyses to find relations between behavioral symptoms, and neuroimaging measures of brain structure and function in adolescence. We found two symptom groups, consisting of anxiety/depression and executive dysfunction symptoms respectively, which correlated with distinct sets of brain regions and inter-regional connections, measured by structural and functional neuroimaging modalities. We found that the neural correlates of these symptom groups were present before behavioural symptoms had developed. These neural correlates showed case-control differences in corresponding psychiatric disorders, depression and ADHD, in independent clinical samples. By characterising behavioral symptom groups based on shared neural mechanisms, our results provide a framework for developing a classification system for psychiatric illness, which is based on quantitative neurobehavioural measures.

Adolescence and its transition toward young adulthood is a critical period for the development of psychiatric illness with half of the lifetime psychopathological burden emerging by the mid-teens, and 75% by the mid-20s[1]. It coincides with major structural changes in grey and white matter[2] that are particularly pronounced in the limbic system and the prefrontal cortex[3]. Cognitive and (other) behavioural maturation reflects this brain-wide developmental process[4]. As psychopathological symptoms during adolescent brain re-organization are often unspecific, and in many cases reversible, it has been difficult to unambiguously identify early markers for sustained mental illness. Thus, most patients present during adulthood, often at a point when severe psychopathology has developed, which gravely impairs their daily functioning. Presentation at this advanced stage increases individual suffering and renders therapeutic interventions more difficult.

Currently, both adolescent and adult psychiatric diagnoses are made on the basis of combinations of behavioural symptoms that - whilst reflecting the psychopathological experience of generations of clinicians and patients - are not necessarily related to homogeneous pathophysiological or etiological processes. This results in biological heterogeneity within diagnostic entities[5] , high rates of comorbidity between diagnoses[6,7], and ill-defined targets for drug development. This is particularly relevant in adolescence, where there is evidence to suggest that psychiatric illness is more dimensional and less categorical than adult psychopathology. Neuroimaging methods offer the opportunity to identify the biological mechanisms underpinning mental illness, without recourse to these categorisations[8,9].

One of the challenges in breaking up diagnostic borders in favour of more homogenous clusters of symptoms sharing common neural mechanisms, is that

biological and behavioral data need to be combined in a meaningful way. A suitable method for this purpose is canonical correlation analysis (CCA), which is formulated to maximize the correlation between variables in two views of a dataset. This technique has previously been used to link complex behavioural datasets with functional brain networks[10]. However, CCA has a number of limitations: It cannot be applied to data with more features than samples, results are difficult to interpret owing to a lack of localizability, and it is only possible to find relations between two sets of variables. The first two of these issues can be addressed using sparse canonical correlation analysis (sCCA)[11,12], which has been used to find modes of shared variation between resting state functional connectivity MRI, and behavioral measures in adolescents and young adults[12]. However, this approach is still limited in that it is only possible to identify relations between psychiatric symptoms and one kind of biological measure at a time. We further enhanced sCCA by formulating a constrained form of multiple canonical correlation analysis, which maximizes the correlation between psychiatric symptoms, and several different neuroimaging modalities simultaneously[13], before combining them in a linear regression model; we term this approach sparse multiple canonical correlation analysis regression (msCCA-regression).

We investigated whether symptoms contributing to DSMV/ICD10 diagnoses can be reconfigured to identify 'neurobehavioral' symptom groups that best represent specific underlying dysfunctional brain networks in adolescence. Here, we used a data driven approach applied to a large general population neuroimaging sample to investigate direct relations between neuroimaging measures of brain structure and function, yet without immediate recourse to diagnostic psychiatric categories. Following this, we sought to determine whether the regions we found to be related to

psychiatric symptoms in adolescence were associated with fully-blown clinical psychopathology in several independent clinical samples. Overall, this multi-step approach enabled us to identify brain correlates of psychopathology in adolescence, probe their predictive value in the critical period between age 14 and age 19, and characterize these brain correlates against the development of full-blown psychopathology.

Results

We used msCCA-regression (please see the methods section under the sub-heading: Multiple Sparse Canonical Correlation Analysis Regression) to link participant responses to the Development and Well Being Assessment (DAWBA), a structured interview for psychiatric DSMV/ICD-10 diagnoses[14] (Supplementary Table 1), with voxel-based morphometry (VBM)[15] measures of grey matter volume, fractional anisotropy (FA) along major white matter tracts using tract-based spatial statistics (TBSS)[16], and functional connectivity between different brain regions, mapped from resting state (rs-fMRI) scans[17]. T_1 and DTI data were pre-processed using voxel-wise VBM[18] and TBSS[19] methods respectively, as these procedures have been extensively studied and applied to real data. We mapped inter-regional rs-fcMRI connections across the brain using nodal maps defined by Miller et al[17], reasons for our pre-processing and analysis choices are detailed in the methods section of the paper under the sub-heading: Different Neuroimaging Pre-processing Strategies. We investigated ninety DAWBA items (symptoms) related to a broad range of psychiatric disorders, including affective and anxiety symptoms, attention deficit/hyperactivity and conduct symptoms, as well as substance use, eating

disorders, and symptoms of psychosis (Supplementary Table 1)[14]. This analysis was carried out on the general population IMAGEN sample, on participants of age 19. Following an in-depth QC (see methods under the sub-heading: IMAGEN analysis), data for n = 666 participants was available at age 19.

To avoid overestimating the variance shared between psychiatric symptoms, and the neuroimaging modalities analysed (overfitting), we used a train/test analysis design, which allows us to estimate effect sizes in an unbiased way. Using a test set also allowed us to carry out further characterization of the data, without running into circularity problems. We carried out model selection in a training dataset of 70% of the data (n=467), and model validation in the testing dataset of the remaining 30% (n=199). To enhance stability we resampled the data and retained only variables that contributed to the model in 90% of resamples (see methods under the sub-heading: Stability Selection, and Supplementary Figure 1)[21]. Demographic information on the full sample, training and testing sets is given in Supplementary Figure 2. The msCCA-regression procedure we used in this investigation is designed to maximise associations between variable-sets. For this reason, all msCCA-regression significance values reported in the text are one-sided.

Using msCCA-regression, we found a significant relation between a subset of six DAWBA symptoms (see Figure 1), and VBM, TBSS and rs-fMRI measures ($r=0.59(465)$, $p<0.001$). The behavioural correlates derived from DAWBA covered symptoms linked to feelings of depression, anxiety and somatic problems, as well as temper and attentional problems (Figure 1). The model was also significant when applied to the test dataset ($r=0.23(197)$, $p<0.001$, 95% CIs=0.13, ∞) (Figure 1), explaining 5.30% of the variance between psychiatric symptoms and the brain. Brain

correlates derived from VBM, TBSS and rs-fcMRI measures were associated with this anxiety/depression symptom group with correlation values of: r=0.16(197), p=0.017, 95% CIs=0.040, ∞; r =0.14(197), p=0.040, 95% CIs=0.037, ∞ and r=0.15(197), p=0.029, 95% CIs=0.041, ∞ respectively (with all p-values FWE-corrected for multiple comparisons, see methods under the sub-heading: Analysis Design, and Supplementary Figure 3).

VBM, TBSS and rs-fcMRI modalities all showed an individually significant relation to psychopathology. We carried out further localization analyses in each modality to identify brain regions that showed an individually significant relation to psychopathology (see methods under the sub-heading: Additional Analyses to Localise Effects). In this localization analysis, we identified one gray matter cluster in the right inferior temporal gyrus (r=0.16(197), p=0.032 FWE corrected, 95% CIs=0.041, ∞), and a single cluster of decreased fractional anisotropy in the genu of the corpus callosum (r = 0.16(197), p=0.031 FWE corrected, 95% CIs=0.041, ∞). Both of these brain regions have been among those exhibiting the largest differences between healthy controls and patients with depression, in recent large, well-powered meta-analyses[22,23]. Further, we found an increase in functional connectivity between the default mode network, and the cerebellum (r=0.15(197), p=0.041 FWE corrected, 95% CIs=0.037, ∞); the default mode network has been implicated in several different psychiatric disorders, but depression in particular, with recent research showing that connectivity between the cerebellum and the default mode network is altered in patients with depression[24]. Information on the full set of regions found to be associated with psychiatric symptoms can be found in Supplementary Tables 2 and 3 and Supplementary Figures 4 and 5.

We then removed the effects of the first canonical relation and investigated the presence of a second dimension of shared variance between symptoms and the brain (see methods under the sub-heading: Finding Multiple Modes of Variation). Here, we identified another behavioral correlate consisting of five items from the DAWBA, including: problems with attention, fidgeting, rapidly changing moods and (lack of) conscientiousness that was significantly associated with the neuroimaging modalities (r=0.46(465), p=0.004). The test sample correlation is significant at (r=0.19(197), p=0.002, 95% CIs=0.087, ∞), explaining 3.61% of the variance between psychiatric symptoms and the brain. Brain correlates derived from VBM, TBSS and rs-fcMRI measures were associated with the executive dysfunction symptom group with correlation values of r=0.19(197), p=0.012, 95% CIs=0.079, ∞; r=0.070(197), p=0.21, 95% CIs=-0.029, ∞ and r=0.020(197), p=0.58, 95% CIs=-0.090, ∞ respectively. These results are displayed in Figure 2.

As the VBM modality was the only modality in this second canonical relation to show an individually significant relation to psychopathology, we only carried out a localization analysis for VBM data in this modality; we found that executive dysfunction symptoms correlated with a single grey matter cluster in the right middle temporal gyrus (r = 0.16(197), p = 0.024 FWE corrected, 95% CIs=0.049), an area that has previously been shown to be associated with ADHD symptomology[25]. Information on the full set of regions found to be associated with psychiatric symptoms can be found in Supplementary Tables 4 and 5 and Supplementary Figures 4 and 5. Associations between canonical anxiety/depression and executive dysfunction canonical correlates are given in Supplementary Table 6. Our results were robust to different rs-fcMRI atlas choices, as shown by repeated analyses using

a different nodal definition[20], which generated similar results (Supplementary Figure 6).

Hypothesis Driven Analysis

To determine if the canonical symptom groups identified in our data-driven analysis show a stronger relation to neuroimaging measures than existing means of organizing psychiatric symptoms, we carried out a hypothesis driven analysis using internalizing and externalizing symptoms, which are often used in adolescent psychiatric diagnostics. We tested whether the canonical symptom groups identified with msCCA-regression were able to explain more variance than this widely used model of illness (see methods under the sub heading: Hypothesis Driven Analysis)[26]. We term these pre-defined symptom groups as DAWBA-internalising and DAWBA-externalising. We found that the correlation of the DAWBA-internalising dimension of psychopathology with neuroimaging measures only shows trend-level significance in the test set ($r=0.12(197)$, $p=0.060$, 95% CIs=-0.02, ∞) and explains 1.9% of variance. Similarly, DAWBA-externalising dimensions of psychiatric illness correlated with neuroimaging measures at ($r=0.040(197)$, $p=0.28$, 95% CIs=-0.095, ∞) in the test set, explaining 0.16% of the variance (Supplementary Figure 7). We then used a modified version of Dunn and Clarke's z[27,28] to test directly whether the association of the canonical symptom groups with the brain was significantly stronger than their pre-defined analogues. While the symptom-brain correlation of the executive-dysfunction symptom group was indeed significantly stronger than that of the DAWBA-externalizing symptom group ($Z=1.95(196)$, $p = 0.029$), we did not find evidence that the strength of the association between the anxiety/depression

symptom group and the brain was significantly larger than that of the DAWBA-internalizing group ($Z=0.92(196)$, $p = 0.18$).

Longitudinal Analysis

We carried out the initial cross-sectional analysis relating psychiatric symptoms to brain at age 19, as most psychopathological symptoms will have become manifest by this age. To investigate how adolescent brain development relates to the development of psychopathological symptoms, we analyzed data from the same participants at age 14 years. First, we repeated the cross-sectional msCCA-regression analysis using VBM and TBSS (rsfMRI data was not available at age 14). We found a non-significant, trend level association between symptoms and neuroimaging measures of $r = 0.42(410)$, $p = 0.11$ in the training set. We found similarly non-significant results in the testing set ($r = 0.10(180)$, $p = 0.090$, 95% CIs=-0.017,∞). The results of these analyses are displayed in Supplementary Figure 8.

There is previous evidence to suggest that neuroimaging measures precede the development of psychiatric symptoms in adolescence[29]. We tested whether that was the case with the canonical symptom groups established in the present study by extracting the TBSS and VBM regions discovered at age 19 and using them as regions of interest at age 14. In order to obtain unbiased estimates of effect, we looked for associations in the test sample. After a conservative quality control procedure (see methods under the sub-headings: Longitudinal Analysis), n = 182 participants were available for analysis at this time-point. Our data did not show any evidence of an association between anxiety/depression brain correlates and anxiety/depression symptoms at 14 years $r=0.020(180)$, $p=0.40$, 95% CIs=-0.10, ∞. However, the brain correlates taken from data at age 14, were predictive of

symptoms at age 19 r=0.14(180), p=0.023, 95% CIs=0.022, ∞. These results are shown in figure 3. The difference in correlation between brain correlates at age 14 years with anxiety/depression symptoms at 14 years and 19 years was also significant, testing for a difference in association using a modified version of Dunn and Clarke's Z (Z=1.74(179), p=0.041)[28]. We did not find evidence of an association between brain correlates and symptoms of executive dysfunction at age 14 years (r=0.030(180), p=0.41, 95% CIs=-0.093, ∞). Prediction of symptoms at 19 years showed a trend towards significance (r=0.11(180), p=0.065, 95% CIs =-0.010, ∞).

Clinical Characterization

We investigated whether the canonical correlates of psychopathology we identified in a general population adolescent sample are correlated with fully developed psychiatric illnesses. In these analyses, we looked for case-control differences in the anxiety/depression and executive dysfunction canonical correlates, across four common psychiatric illnesses in several independent clinical samples. We carried out these analyses using VBM data alone, as this was the only data modality that showed an individually significant association with both symptom groups. Clinical and demographic information associated with the different clinical samples is displayed in Supplementary Figure 9 and Supplementary tables 7-9. Extensive information on quality control and data exclusion criteria for these clinical samples is given in the methods section of this paper following the sub-heading: Clinical

Analyses. In assessing this data, we were looking for a directional effect, we therefore report significance levels resulting from one-tailed tests in this section of the paper.

When analyzing the data for case-control differences in grey matter correlates of anxiety/depression symptoms, we found significant reductions in regional grey matter volume in independent samples of patients with Depression (t-statistic=4.61(612), $p<0.001$, Cohen's D = 0.39, 95% CIs=0.25, ∞), Schizophrenia (t-statistic=2.54(445), p=0.002, Cohen's D=0.25, 95% CIs = 0.087, ∞) and in ADHD (t-statistic=1.84(203), p=0.034, Cohen's D=0.26, 95% CIs=0.030, ∞). In the executive dysfunction grey matter correlates, we found significant differences between patients and healthy controls in ADHD (t-statistic=2.19(203), p=0.014, Cohen's D=0.32, 95% CIs=0.070, ∞), Schizophrenia (t-statistic=2.84(445), p=0.0026, Cohen's D=0.28, 95% CIs=0.11, ∞) and Depression (t-statistic=1.65(612), p=0.050, Cohen's D=0.14, 95% CIs=0.001, ∞). We did not find significant effects of bipolar disorder along either of these dimensions (t-statistic=-0.23(473), p=0.59, Cohen's D=-0.02, 95% CIs=-0.17, ∞) and (t-statistic=-1.33(473), p=0.90, Cohen's D=-0.12, 95% CIs=-0.27, ∞) respectively (Figure 4). In these case-control analyses, the data distribution was assumed to be normal but this was not formally tested. To test whether the observed reduction in grey matter was specific to the brain correlates identified, as opposed to being a proxy for a generalized, brain-wide reduction in grey matter, we repeated the clinical comparisons using total grey matter as a covariate of no interest in addition to total intracranial volume (Supplementary Figure 10). ADHD and Depression results were unaffected by this change in pre-processing. In contrast, the Schizophrenia results were no longer significant.

Discussion

We ran analyses to establish direct relations between psychiatric symptoms and neuroimaging measures of brain structure and function, without immediate reference to pre-defined psychiatric categories. This kind of dimensional, data-driven, approach is particularly relevant in adolescence where there is a good deal of evidence suggesting that psychopathology is less differentiated than in adulthood and therefore doesn't fit into the traditional categorical conception of psychiatric disorder[30,31]. We find two largely non-overlapping sets of brain regions that correlate with different sets of psychiatric symptoms. The first symptom dimension predominantly encompassed anxiety/depression symptoms whilst the second dimension mainly consisted of executive dysfunction symptoms.

The anxiety/depression canonical symptom correlate was significantly associated with T_1, rs-fcMRI and DTI data modalities. Participants scoring highly on this psychiatric scale showed decreased grey matter volume in the middle temporal gyrus, reduced fractional anisotropy in the genu of the corpus callosum, and increased functional connectivity between the default mode network and the cerebellum. A recent meta-analysis has demonstrated an association of depression with the right inferior temporal gyrus[22], a region exhibiting close connections with the limbic system, consistent with the theory that depression results from dysfunctional cortico-limbic circuits[32]. The genu of the corpus callosum is a commisural white matter pathway that links left and right prefrontal brain regions[33]. Changes in the structure of the corpus callosum are known to result in altered inter-hemispheric connectivity and impaired emotional control[34]. The genu of the corpus callosum has been shown to be the white matter region with the largest difference in FA between

controls and patients with major depression[35]. The default-mode network is a set of brain regions that reliably exhibit a decrease in activity when the brain is engaged in non-self-directed tasks; this network is thought to be primarily responsible for self-inspection and internal monitoring[36,37], which are processes overactive in depression[38]. Increased connectivity between the default-mode network and the cerebellum has been previously reported in drug-naive depressive patients[24], consistent with its recently discovered involvement in complex cognitive and emotional processes[39].

We found that the executive dysfunction psychiatric symptom group was significantly correlated with neuroimaging measures derived from T_1 data. Here, decreased grey matter was localised to the Right Middle Temporal Gyrus, previously linked to ADHD[25]. These results are more difficult to interpret as the function of this brain area is not well studied. As with the rest of the temporal lobe, this brain area is thought to be responsible for generating meaning from sensory inputs[19]. Further, the temporal lobe functions in close relation with the hippocampus in the formation of memories[19]. Therefore, atrophied grey matter in this brain area may help explain the learning deficits often observed with ADHD-like symptoms.

The identification of brain systems from a population-based cohort that is not suffering from any other psychiatric illness has major advantages: By identifying sub-clinical correlates of psychiatric illness, prior to the full manifestation of disorder, it is possible to avoid the potential impact of effects indirectly related to illness, such as substance use and medication effects. For example, 17% percent of the schizophrenia, and 21% percent of the Bipolar samples but none of the healthy controls studied here have a history of alcohol abuse, which has been linked to widespread decreases in grey matter[40]. In addition, various psychiatric medicines,

424 including lithium, which is often prescribed to Bipolar patients, have also been linked
425 to alterations in grey matter volume[41], it is possible that lithium-induced increases in
426 grey matter volume may have contributed to the observed absence of significant
427 findings in Bipolar patients in this study.

428 We compared the efficacy of the data-driven msCCA-regression method with
429 pre-defined psychiatric scales of internalising and externalising symptoms. We found
430 that the data driven approach identified relations between symptoms and the brain
431 that were significantly stronger than a similar approach using standard internalising
432 and externalising psychiatric symptom scales, defined without reference to any
433 underlying biology. The fact that the canonical symptom groups show a stronger
434 correlation with neuroimaging measures than pre-defined scales is important as it
435 shows that data driven methods may offer the potential to refine existing psychiatric
436 categorisations[6].

437 It is notable that grey matter correlates of psychopathology are already
438 present at age 14 years, preceding the development of symptoms that only become
439 manifest 5 years later, at 19 years. We also found that the brain correlates
440 identified in the adolescent general population replicate in independent clinical
441 samples of corresponding psychiatric disorders, namely depression and ADHD. In
442 addition to validating our primary results gained from population cohorts, these
443 results raise the prospect of using neuroimaging measures, discovered in preclinical
444 samples, as predictors of future psychopathology, thus enabling the development of
445 targeted interventions in a young age group, where such measures are most
446 effective in reducing the burden of mental illness[42].

447 It is important to note that the results of the msCCA-regression analysis
448 applied here, depend on the distribution of prevalence of psychopathological

symptoms in each sample investigated. Thus, while a general population sample may yield an index of the normative variance in psychiatric symptoms from a broader range of different psychiatric disorders and their neural correlates, a patient sample might yield a narrower biological stratification within distinct clinical psychiatric categories, e.g. different biotypes of depression[5], or symptoms of psychosis.

By basing symptom groups upon brain correlates, and by demonstrating specific associations of these correlates with clinical psychopathology, we have characterized stratification markers based on shared neural substrates. By discovering that these brain correlates identified in young adults are already established during adolescence, we have characterized biological risk markers prior to the manifestation of symptoms. Our work thus shows how major obstacles can be overcome in developing a taxonomy for psychiatric illness based on quantifiable neurobehavioral phenotypes.

Methods

Ethics Statement

IMAGEN

Each site sought and received approval from the relevant local research ethics committee. Written consent was obtained from each participant and a parent or guardian.

Munich-Depression

The studies were approved by the respective local ethics committees: The ethical committee of the Ludwig-Maximilians-Universität, Munich, Germany and the ethical committee of the Bayerische Landesärztekammer, Munich, Germany. All participants provided written informed consent.

TOP

All participants were recruited between 2003 and 2009 as part of an ongoing study of psychotic disorders (Thematically Organized Psychosis study). After complete description of the study, all participants gave informed consent to participate. The

study was approved by the Regional Committee for Medical Research Ethics and the Norwegian Data Inspectorate.

ADHD

This study was approved by the regional ethics committee (Centrale Commissie Mensgebonden Onderzoek: CMO Regio Arnhem – Nijmegen; 2008/163; ABR: NL23894.091.08) and the medical ethical committee of the VU University Medical Center. Informed written consent was obtained from each participant. For children under 18, both parents and children gave consent.

Study Protocol

We developed a method, termed msCCA-regression to find multivariate relationships between psychiatric symptoms, and multiple neuroimaging modalities simultaneously; In this case, voxel-based morphometry (VBM)[18] measures of grey matter volume, fractional anisotropy (FA) derived from DTI data, and normalized using tract based spatial statistics (TBSS)[19], and resting state functional connectivity neuroimaging measures[43]. msCCA-regression analysis was carried out in the general population IMAGEN sample, when participants were aged 19. Additional analyses were then applied in order to localize associations between psychiatric symptoms, and neuroimaging measures of brain structure and function. We then analyzed neuroimaging and symptom data at age 14 in order to determine whether this multivariate relationship already existed at this earlier time-point. Following this, we assessed the clinical significance of our findings by conducting case-control comparisons of the structural markers found in the IMAGEN analysis, in several clinical samples. The following text gives a more detailed description of the methods described here.

IMAGEN Analysis

IMAGEN is a large-scale neuroimaging-genetics cohort study conducted with the aim of understanding the biological basis of individual variability in psychological and behavioural traits, and their relation to common psychiatric disorders[44]. The study involves a thorough neuropsychological, behavioural, clinical and environmental assessment of each participant. Participants also undergo biological characterisation, with the collection of T_1 weighted MRI (sMRI), diffusion tensor imaging (DTI), task-based fMRI (t-fMRI), resting-state fMRI (rs-fcMRI) and genetic data. We used T_1 weighted, DTI, and rs-fcMRI data in the current investigation.

Participants

The analysis was carried out on participants drawn from the IMAGEN sample (see for further details: Schumann et al[44]. For IMAGEN, a general population sample of Caucasian adolescents were recruited from eight sites across France, Ireland, England and Germany. Data was collected at age 14, 16 and 19 years. After a conservative quality control of MRI acquisitions and DAWBA questionnaires, participants with complete data were used in the subsequent data analysis. No statistical analyses were used to pre-define sample size. However, the sample size used was simlar to that reported in previous studies[10,12].

DAWBA

Psychiatric symptoms of the IMAGEN participants were assessed using screening questions from the development and wellbeing assessment (DAWBA), a wide ranging psychiatric screening questionnaire[45]. Participants were asked screening questions, assessing symptoms of: specific fears, social fears, stress after a very

frightening event, obsessions and compulsions, worrying, depression, rapidly changing mood, attention and activity, troublesome behavior, drug and alcohol use, concern about appearance and strange/frightening experiences; if enough of these questions were answered in the affirmative, a more in-depth assessment of symptoms associated with that disorder was made. DAWBA screening questions have previously been used to define subthreshold clinical symptoms in neuroimaging studies of subclinical psychopathology[46]. The strength and difficulties questionnaire (SDQ) was also used in the present investigation as this questionnaire contributes to the assignment of diagnostic status in the DAWBA[45]. Questions in the SDQ are categorized into broad internalising and externalizing domains. The data of four of the questions asked had a standard deviation of zero amongst the participants asked, and were therefore not used in subsequent analyses. The full set of psychiatric questions asked in the present investigation can be found in Supplementary Table 1, the questionnaire items that were omitted from the analysis are marked here. At the time of the analysis conducted here, DAWBA/SDQ data had been collected for 1510 participants. Of these, data was incomplete for 239 participants, and was not used.

T_1 Weighted MRI Acquisition

Scanning took place at eight different sites across Europe, using scanners built by four different manufacturers (Siemens, Philips, General Electric, Bruker). High resolution, T_1 weighted images were obtained using a Magnetization Prepared Rapid Acquisition Gradient Echo (MPRAGE) sequence, based on the ADNI protocol (http://www.loni.ucla.edu/ADNI/Cores/index.shtml). Scan parameters were standardized across sites to the highest degree possible (sagittal slice plane;

repetition time: 2.3 s; echo time 2.8 ms; flip angle 8°; 256×256×160 matrix; isotropic voxel size: 1.1 mm).

VBM Pre-processing

At the time this investigation was conducted, T_1 data had been acquired for 1400 participants. All scans were visually inspected and manually reoriented. 285 scans were discarded from the analysis for either movement artifacts, strong field inhomogeneities, abnormal field of view, abnormally reduced cerebellum and for brace artefacts. The resulting 1,115 scans were used to build the study specific template. Baseline and Follow up two scans were preprocessed using both the 2008 version of the Voxel Based Morphometry toolbox (VBM8) running in SPM8 (v.5236). Given the young adults recruited in IMAGEN, we first used VBM8 in order to avoid using adult tissue probability maps (TPM) to initiate the segmentation process. The VBM8 toolbox segmentation relies on an adaptive Maximum a Posterior technique and TPMs used in VBM8 are for registration purposes only. Diffeomorphic registration (Dartel) was then used to register the 1,115 images, and to generate the study-specific population average template[47]. We then resliced the data to 1.5x1.5x1.5mm voxel size. Smoothing was carried out using an isotropic 8 mm full width at half maximum Gaussian smoothing kernel. We created a mask for the sample by taking the mean across all VBM maps included in the sample. We thresholded the mask at >0.4. We used a stringent mask to avoid overfitting the data[48]. We then extracted all voxel values within this mask, resulting in 241,544 grey matter voxels.

DTI Acquisition

Diffusion tensor imaging acquisition sequence based on the study by Jones et al[49]. Diffusion tensor images were acquired using an Echo Planar imaging sequence (b=0 and 32 directions with b-value 1300 s/mm^2; axial slice plane; echo time = 104ms; 128x128x60 matrix; voxel size 2.4x2.4x2.4 mm), adapted to tensor measurements (for example, FA, mean diffusivity (MD)) and tractography analysis.

TBSS Pre-processing

At the time this study was conducted, DTI data had been acquired for 1412 participants. Of these, 71 were not usable due to: signal dropouts or too much rotation. Diffusion imaging data was pre-processed using software from the FSL toolbox (www.fmrib.ox.ac.uk/fsl)[50]. We preprocessed the remaining 1341 scans using tract based spatial statistics (TBSS)[19]. Pre-processing was carried out in the following manner: An affine registration was applied to the first B_0 image for head motion and eddy current correction. Brain extraction was carried out using BET. Diffusion tensor fitting was then used to obtain fractional anisotropy (FA) maps for each participant. All participants' FA data was aligned into a common space using the non-linear registration tool FNIRT, using a b-spline representation of the registration warp field. The mean was then taken across all FA maps to create an FA averaged image. This map was then 'thinned' to create a mean FA skeleton, which was then thresholded at FA > 0.2, keeping only the major white matter tracts. Each participant's aligned FA data was then projected onto the mean skeleton. We then used these skeletonised maps in all subsequent analyses. The final mask used contained 106,812 voxels. A further 10 scans were not used due to masking or normalization issues in TBSS.

Resting State fMRI Acquisition

Resting state fMRI scanning of the IMAGEN participants was carried out at multiple sites. The following parameters were standardized: number of volumes (164), TR = 2.2s, TE = 30ms, flip angle = 75, number of slices/ddas = 40/3, slice thickness = 2.4 mm, slice gap = 3.4 mm, voxel size = 3.4 x 3.4 x 2.4 mm^3, matrix size = 64^2, FOV = 218 mm.

Resting State fMRI Preprocessing

At the time of this investigation, we had collected rsfMRI scans for 1067 participants. Of these scans, 157 were not used, either because over 5% of scans in that participant exhibited artifacts of some kind, or if over 5% of volumes showed a fractional displacement of over 0.5mm. Preprocessing of resting-state data was performed with routines from FMRIB's Software Library (FSL v5.0.9)[50] and Advanced Normalization Tools (ANTs v1.9.2)[51].

1) Motion correction was carried out, applying a rigid body registration of each volume to the middle volume (FSL MCFLIRT).

2) Non-brain tissue was removed (FSL BET).

3) Spatial smoothing was applied using a 5mm FWHM Gaussian kernel.

4) Independent component analysis (FSL MELODIC) was run for each data set. Artifact components were identified using an automatic classification algorithm, and subsequently regressed from the data (ICA-AROMA v0.3)[52,53]. ICA-AROMA[52] has been shown to be as effective as motion parameter regression, with additional spike regression and 'scrubbing', in the removal of

motion related effects on functional connectivity measures derived from resting state fMRI data. However, this procedure has the additional benefit that it preserves more signal of interest than these methods[53.]

5) The resulting cleaned data set was de-trended (up to a third degree polynomial).

6) Co-registration to a high-resolution T_1 image (FSL FLIRT using the BBR algorithm), and normalization to 2mm isotropic MNI standard space (ANTs) was carried out.

7) We used the CompCorr procedure to further clean the data of physiological noise[54]. To do this: we created white matter (WM) and cerebrospinal fluid (CSF) masks by taking the mean of the WM and CSF segmentations from the VBM analysis, and thresholding them at 0.95, we then resliced these maps into the same space as the rsfMRI data. We then extracted timecourses from voxels within these regions, and took the first three principal components of this signal for both WM and CSF maps. These six principal component signals should represent non-neuronal signal. We then regressed this non-neuronal signal from voxel timecourses across the rest of the brain.

8) Lastly, preprocessed and normalized resting-state data sets were resliced to 3mm isotropic voxels.

Mapping rs-fMRI data

1) We first generated 55 regional nodal timecourses using dual regression on nodal regions established in the UK biobank sample[17].

2) We mapped the correlation between nodal regions using Pearson's pairwise correlation coefficient, for each participant, thus producing a connectivity matrix for each participant. This connectivity matrix consists of 1,485 connections between nodes.

3) We then transformed these connectivity values using Fisher's Z-score transform.

Different Neuroimaging Processing Strategies

A wide range of different preprocessing strategies can be applied in the analysis of neuroimaging data. Approaches to analysing DTI and T1 can be categorised into two broad types: voxelwise, and atlas based approaches[18,55]. We chose to analyse this data at the voxelwise level, as this allows for the highest level of spatial specificity. Although it is also technically possible to analyse rs-fcMRI data across the whole brain at the voxelwise level, this approach results in an enormous number of features: When mapping connectivity at the voxelwise level, in a dataset made up of N voxels, we are left with (N*(N-1))/2 connections between those voxels. In the current investigation, N = 57,053, leading to N*(N-1)/2 = 1.63 billion inter-regional connections. This would lead to a huge amount of redundancy in the data and computational, statistical and interpretational issues. For this reason, we mapped the connectivity between a pre-defined set of nodes. We used nodal definitions resulting from previous work applying independent component analysis (ICA) to the UK biobank sample[17]. We used this nodal definition as it derives from the largest extant sample of neuroimaging data. In order to test whether the results we obtained were

robust to different nodal definitions, we also mapped inter-regional connectivity using the widely used Power atlas[56] and achieved similar results (Supplementary Figure 6).

Canonical Correlation Analysis and Sparse Canonical Correlation Analysis

Canonical correlation analysis (CCA) is a very general statistical method used to identify linear relationships between two or more sets of variables[57]. It can be thought of as a generalization of multiple linear regression. The objective of CCA is to identify a relationship between two (or more) sets of variables, where there is no distinction between which variables are considered dependent, and which are considered independent. This method identifies weights for each variable, such that the weighted sum of variables in each set is maximally correlated with the weighted sum of variables from the opposite set, assuming a linear relationship.

Consider two matrices $\boldsymbol{X}_1$and $\boldsymbol{X}_2$, where each row denotes one of *n* observations, and each column denotes one of p_1 *or* p_2 features. CCA seeks to find the weight vectors $\boldsymbol{w}_1$ and $\boldsymbol{w}_2$ that maximise the correlation:

$$\rho = corr(\boldsymbol{X}_1\boldsymbol{w}_1, \boldsymbol{X}_2\boldsymbol{w}_2).$$

This optimisation problem can be written as:

$$\rho = max_{\boldsymbol{w}_1,\boldsymbol{w}_2}\, \boldsymbol{w}_1^{\boldsymbol{T}}\boldsymbol{X}_1{}^{\boldsymbol{T}}\boldsymbol{X}_2\boldsymbol{w}_2$$

Subject to the constraints:

$\boldsymbol{w}_1^{\boldsymbol{T}}\boldsymbol{X}_1{}^{\boldsymbol{T}}\boldsymbol{X}_1\boldsymbol{w}_1 = 1$ and $\boldsymbol{w}_2^{\boldsymbol{T}}\boldsymbol{X}_2{}^{\boldsymbol{T}}\boldsymbol{X}_2\boldsymbol{w}_2 = 1$.

We assume that the columns of $\boldsymbol{X}_1$ and$\boldsymbol{X}_2$ have been standardised to have a mean of zero and a standard deviation of one. The vectors $\boldsymbol{X}_1\boldsymbol{w}_1$ and $\boldsymbol{X}\boldsymbol{w}_2$ are referred to as canonical variates.

Classical CCA is extremely powerful, but cannot be applied in situations where there are a more features than samples (i.e., $p_1 > n$ or $p_2 > n$, which is typically the case in neuroimaging studies). Interpreting and describing results from CCA can be difficult because the estimated weights are not sparse. This means that some variables may make negligible but non-zero contributions to the variance explained between sets. Sparse canonical correlation analysis (sCCA) was developed to address these issues[11,58,59].

sCCA uses an L_1 penalty on canonical weights, which forces some of them to take a value of exactly zero. Furthermore, sCCA can also be applied in scenarios where there are more features than samples ($p > n$). The optimization criteria for sCCA can be written in the following manner:

$$\rho = max_{\boldsymbol{w}_1,\boldsymbol{w}_2} \boldsymbol{w}_1^T \boldsymbol{X}_1{}^T \boldsymbol{X}_2 \boldsymbol{w}_2$$

Subject to the constraints:

$\|\boldsymbol{w}_1\|^2 = 1$, $\|\boldsymbol{w}_2\|^2 = 1$, $\|\boldsymbol{w}_1\|_1 \leq c_1$ and $\|\boldsymbol{w}_2\|_1 \leq c_2$

Here, c_1 and c_2 are assumed to fall within the bounds $1 \leq c_1 \leq \sqrt{p_1}$ and $1 \leq c_2 \leq \sqrt{p_2}$, where p_1 and p_2 are the number of features in views X_1 and X_2 respectively.

Multiple Sparse Canonical Correlation Analysis Regression

The formulation of sparse canonical correlation analysis described in the text above is designed to find relations between two views of a dataset. However, we have

collected data from several different neuroimaging modalities, and would like to utilize information from each of them. A somewhat naive approach to finding relations between psychiatric symptoms and multiple neuroimaging measures would be to include all available neuroimaging modalities in one view of the canonical relation, with psychiatric symptoms in the other view. However, this approach is likely to be problematic as different modalities are associated with very different numbers of features. For example, the functional connectivity data used in the present investigation has only 0.6% of the number of features that the VBM data has. As such, if these modalities were entered into the same model, the VBM data would overwhelm the functional connectivity data.

We developed an approach designed to maximise the cross-correlation between psychiatric symptoms, and multiple neuroimaging modalities simultaneously, we then combined these modalities in a linear regression model. Formulations of canonical correlation analysis that are able to find relations between more than two sets of data are termed multiple or generalised canonical correlation procedures. A widely used optimisation criteria for multiple canonical correlation analysis is to maximise the sum of correlations between each of the different views of a dataset[60]. Witten et al have formulated a sparse version of multiple canonical correlation analysis[58]; this formulation is designed to maximise the sum of correlations between all views of the data. However, in the present investigation, we are only interested in finding correlations between neuroimaging measures, and psychiatric questionnaire responses; we do not wish to optimise the correlation between different neuroimaging measures.

As such, we seek to maximise the following relation:

$$max_{\boldsymbol{w_1,..,w_n}} \boldsymbol{w}_1^T \boldsymbol{X}_1{}^T \sum_{\boldsymbol{i=2}}^{\boldsymbol{n}} \boldsymbol{X_i w}_i$$

Subject to the constraints:

$\|\boldsymbol{w}_1\|^2 = 1$, $\|\boldsymbol{w}_i\|^2 = 1$, $\|\boldsymbol{w}_1\|_1 \leq c_1$ and $\|\boldsymbol{w}_i\|_1 \leq c_i$

This method simultaneously optimizes the correlation between a weighted sum of variables in the target set, X_1, with a weighted sum of variables in the other sets. In the present investigation, X_1 is a matrix of psychiatric symptoms and X_2 to X_n are neuroimaging measures of brain structure and function. Using this method, we are able to maximise the correlation between psychiatric symptoms, and several different neuroimaging modalities within the same integrated model. A natural choice for the statistic of interest, in any inference carried out using this procedure, would be the sum of correlations between the symptom data, and the neuroimaging measures of brain structure and function. However, a sum of correlations is of less practical benefit than understanding how much total variance is shared between neuroimaging measures of brain structure and function, and psychiatric symptoms. Therefore, in the final step of this process, we combine canonical neuroimaging variables in an ordinary linear regression model. Canonical variables are defined as:

$$C_i = X_i w_i$$

761 Canonical variables are then combined in the prediction of psychiatric symptoms
762 using ordinary linear regression:

$$C_1 = \beta_0 + C_2\beta_2 \ldots + C_n\beta_n + \epsilon$$

763 We used this approach to establish relations between psychiatric symptoms (C_1),
764 and TBSS (C_2), VBM (C_3), and connectivity measures (C_4) derived from rs-fMRI data
765 and β_n are the associated weights estimated using ordinary linear regression (β_0 is
766 the constant estimated in regression).

767 msCCA-regression was carried out using in-house codes written in MATLAB. This
768 algorithm requires an initialization value. In the present study, initial weights were
769 randomly generated**.** Weight values associated with psychiatric symptoms were
770 always constrained to be positive to ensure interpretability.

771 This study is designed to be exploratory in nature. Nevertheless, given the very large
772 quantity of data we sought to integrate, it is likely that some simple priors will help to
773 improve the stability of our results, so long as those priors are well supported. There
774 is a great deal of evidence suggesting that psychopathology is associated with
775 decreases in both grey matter, and fractional anisotropy, across psychiatric
776 disorders[61,62]. For this reason, we constrained the canonical weights on VBM volume
777 and FA to be negative. This will help to reduce variance in the model and will help
778 increase interpretability of our results. In contrast, there is no clear evidence that
779 psychiatric illness is associated with increases or decreases in connectivity
780 measures derived from BOLD-fMRI. Therefore, we did not add constraints to the
781 functional connectivity data.

782

Stability Selection

Although msCCA-regression (and sCCA) have advantages over classical CCA in terms of interpretability, it can suffer from instabilities due to their utilization of an L_1 penalty to introduce sparsity[21]. This is particularly true when $p >> n$, and when there is a high degree of collinearity in the data. Stability selection is a widely applicable feature selection procedure that can address this problem[21]. This procedure has the added benefit that it makes the results less sensitive to the choice of L_1 penalty.

The conceptual underpinning of stability selection is very simple: if a model is repeatedly resampled, features exhibiting a 'real' effect will be selected more often than noise. Using stability selection, data is repeatedly split into random sub-samples of size $n_t/2$ (where n_t is the total number of participants in the training dataset). In this work, resampling was carried out a hundred times. msCCA was applied to each resample, and those features that appear more often are deemed to be more stable. Deciding which variables are stable requires a threshold: π_r is defined as the fraction of samples in which a particular variable must be observed to be considered stable. We set π_r to 0.9, which means that a particular variable must be present in 90% of resamples to be considered stable. The outcome of this stability selection procedure is a set of stable features. A benefit of stability selection is that it is insensitive to tuning parameters. Here, we simply set the L_1 penalty at $\sqrt{p}/2$, which is halfway along the regularization path running from 1 to $\sqrt{p}$. It is worth noting that the stability selection procedure is easily parallelizable here as it simply involves re-applying the msCCA-regression algorithm to multiple different resamples of the same data.

Analysis Design

The L_1 penalty used in sCCA means that the parametric tests used for significance testing in classical CCA (for example Wilk's Lambda)[63] cannot be used here, necessitating the use of permutation testing to determine whether results are significant. We assessed the in-sample significance of the results we obtained here, then replicated these findings using an out-of-sample, hold-out set design. This kind of experimental design has a number of advantages in the present context: using a training/testing design, it is possible to obtain an unbiased estimate of effect size. We used a hold-out set design in preference to a cross-validation procedure. This is because cross-validation involves the training and testing of multiple statistical models, one for each cross-validation fold, which precludes the use of a single model for further validation/characterization. A related advantage is that it is possible to carry out further characterization of the test set results, due to the fact that we are able to estimate effect size in an unbiased way.

In detail, the analysis design was carried out as follows:

1) Psychiatric symptom data, and data from the VBM, TBSS and rs-fcMRI neuroimaging modalities was extracted and transformed into n_t x p_i matrices, where n_t is the number of participants included in the training dataset, and p_i is the number of features included in each of the views of the data.

2) The full dataset was randomly split into training and testing sets. The training set was made up of 70% of the data whilst the testing set was made up of the remaining 30%.

3) The training data was then randomly split into a hundred further resamples. Each resample was made up of $n_t/2$ participant scans, where n_t is the total number of participants in the training dataset.

4) The first stage of the mSCCA- regression algorithm (see above) was then applied to each resample, with a sparsity constraint of $\sqrt{p_i}/2$ in each view of the data.

5) We then recorded which variables, in each view of the data, are present in over 90% of resamples. These variables are considered to be stable, and are retained.

6) We then re-applied the msCCA algorithm to the data, without sparsity constraints, on the variables than survived more than 90% of resamples.

7) We then combined the neuroimaging canonical variates we found in the previous step in a prediction model on the symptom canonical variate, using ordinary least squares regression. We then recorded the correlation between the neuroimaging prediction model, and the symptom canonical correlate.

8) We then permuted the training data, and repeated steps 3-7. This was done for 10,000 different permutations of the training data labelling. In each case, we recorded the correlation between the neuroimaging model, and the canonical correlate of psychiatric symptoms. In this way, we built up a permutation distribution to assess the significance of the relation between symptom and neuroimaging data in the experimental labelling, within the training dataset.

9) We then applied the trained model to the test set to produce canonical correlates of symptom and neuroimaging measures. We recorded associations for both the full model, and between the psychiatric symptom score, and each of the individual neuroimaging canonical correlates.

10) We then randomly permuted the data rows in the testing set and re-calculated correlation values between symptom and brain canonical correlates. We recorded associations between psychiatric symptoms and the full neuroimaging model, for each of 10,000 permutations of the experimental labelling.

11) It is also interesting to find the significance of the individual neuroimaging modalities. However, as we are testing the significance of multiple neuroimaging modalities, it is necessary to correct for multiple comparisons across these different modalities. This is easily done using the distribution of the maximal statistic: for each permutation of the experimental labelling, we calculate the association between the symptom score and each of the neuroimaging canonical correlates; the largest of these associations is then recorded. This is done for each of the 10,000 permutations of the test labelling, producing a distribution of the maximal statistic. Correlations between symptom and neuroimaging measures in the experimental labelling are then significant at the FWE-corrected level α if they are above the 100*(1-α) percentile of this distribution.

This process is illustrated in Supplementary Figure 1.

Confounds

It is important to account for the effects of confounds, which might otherwise lead to spurious relations between the different data views[64]. Here, we regressed age, gender, site and intracranial volume from all data views prior to the sCCA analysis[65-67]. For the connectivity measures derived from rsfMRI data, we also regressed the mean between-volume fractional displacement, and the percent of slices corrupted by artefacts, from the scans.

Additional Analyses to Localise Effects

We used msCCA-regression to find multivariate relations between psychiatric symptomatology and neuroimaging measures of brain structure and function. In using msCCA-regression, it is possible to make inferences on relations between sets of psychiatric symptoms and neuroimaging measures across the brain, it is not possible to make inferences on individual brain regions/connections or individual questionnaire items. For this reason, we conducted additional analyses to further deconstruct the relationship between psychiatric symptomatology and the brain. This procedure is similar to a redundancy analysis[68,69]. In particular, we were interested in localising which brain regions exhibited an individually significant association with psychiatric symptomatology.

Conducting further tests on the whole dataset would introduce circularity into the analysis. Therefore, additional inference must be carried out on the testing dataset alone. Nevertheless, the training dataset is still likely to contain useful information, which can be used to guide analyses carried out on the testing dataset, thus decreasing the multiple comparison problem, and increasing the likelihood of finding significant effects in the testing dataset. In the present investigation, we looked for

significant localizable effects in the training dataset, we then used these results to inform analyses carried out on the testing dataset. In this sense, the training dataset was used as a 'discovery dataset'.

In the case of the TBSS and VBM data, we sought to localize associations between symptoms and the brain to the cluster-wise level. In the case of the rs-fcMRI data, we sought to localize changes to individual inter-regional connections. VBM and TBSS clusters were defined using an 18-connectivity scheme. This means that voxels must be connected by a face or an edge to be considered a part of the same cluster.

This analysis was carried out in the manner described below:

1) We calculated the grey matter volume and FA in spatially distinct clusters identified in the sCCA analysis applied to VBM and TBSS respectively. We extracted connectivity values with non-zero canonical weights. This was done in both the training and testing datasets.

2) We calculated Pearson's correlation coefficient between the mean of each spatially distinct cluster/connection, and the sum of symptom score values. This was done separately in the training and testing datasets.

3) Rows associated with neuroimaging data in the training set were permuted and correlations between clusters/connections, and symptom clusters were recalculated. The maximal value was recorded. Training data was permuted 10,000 times; the maximum correlation value across all clusters/connections was recorded for each permutation. Clusters/connections exhibiting a significant effect in the training dataset were then determined by comparing

correlation values to the distribution of the maximal statistic[50, 51]. Because model selection was carried out in the training dataset, conducting inference on the training dataset would constitute “double dipping”.

4) Clusters/connections exhibiting a significant effect in the training dataset were taken forward for an analysis carried out in the testing set.

5) We calculated correlation values between clusters/connections in the testing dataset, and the symptom score.

6) Testing data was permuted 10,000 times; the maximum correlation value across all clusters/connections was recorded for each permutation. Clusters/connections exhibiting a significant effect in the testing dataset were determined by comparing correlation values to the distribution of the maximal statistic. Cluster/connection correlations in the testing dataset were then compared to correlations in the distribution of the maximal statistic. Cluster/connection correlations in the experimental labelling, which were in the top 5% of the distribution of the maximal statistic, were considered significant at the FWE corrected level.

This process is illustrated in Supplementary Figure 3.

Finding Multiple Modes of Variation

Using canonical correlation analysis, it is possible to uncover multiple modes of variation between datasets. After determining the significance of the first canonical correlate, we remove the effect of the first set of canonical vectors, and repeat the analysis. Witten et al used Hoteling’s deflation to remove the effect of the first vector; this approach has been criticized by Monteiro et al, who propose the projection

deflation procedure as an alternative[11,70]; this is the procedure we use in the present investigation. Correlations between the different canonical relations are given in Supplementary Table 6.

It is possible to ascertain the significance of all canonical relations after the first by comparing the correlations of subsequent associations to the permutation distribution of the first relation: The first canonical relation between sets is by definition the strongest; any subsequent associations between sets will be weaker than the canonical relation that preceded it. A common means of correcting for multiple comparisons is to compare test statistics in the experimental labelling to the maximal statistic across all tests in the permutation distribution; this distribution is usually termed the distribution of the maximal statistic[71,72]. In the present investigation, we can find this distribution by recording the strength of the first canonical relation, for each permutation. Significance values that are corrected for multiple comparisons can then be found by comparing associations of subsequent modes of variation, with this distribution[73].

Hypothesis Driven Analysis

A major advantage of the approach described here is that it allows the grouping of psychiatric illnesses to be driven by their biological underpinnings. Nevertheless, it is an open question whether the symptom groups discovered in the data driven analysis we ran here show a stronger relation to neuroimaging measures of brain structure and function than pre-defined symptom groups. For this reason, we tested whether the widely used internalising/externalising organisation of psychiatric illness is able to explain as much variance in psychiatric symptomatology as this purely data driven method. To do this, we used an approach that is as similar as possible to the

primary data analysis followed in the main part of the investigation, yet still makes use of the internalising/externalising illness structure: we replaced the symptom matrices used in the main part of the investigation with symptom vectors based on previously defined internalising and externalizing symptom sub-scales from the DAWBA; no sparsity was applied to psychiatric symptom sub-scales. Used in this manner, the msCCA-algorithm reduces to something like a sparse partial least squares regression[74], where the neuroimaging features are predictors and the pre-defined internalising/externalising vectors are the targets. This method was applied twice, once to predict the internalising symptom dimension, and once to predict the externalising. We term the internalizing and externalising symptom scales as DAWBA-internalising and DAWBA-externalising respectively. We defined symptoms as belonging to broad internalising or externalising categories in the same way as Aebi et al[75] : The DAWBA-internalising scale was created by summing: specific fears, social fears, panic attacks, stress after a frightening event, worrying and depression. The DAWBA-externalising scale was created by summing: Attention and activity, behaviours and attitudes that can get people into trouble, and Cigarettes, Alcohol and Drugs sections of the DAWBA. The SDQ is already split into broad internalising and externalising domains[45]. Therefore, internalising and externalising SDQ scores were simply added to these scores to create DAWBA-internalising and DAWBA-externalising scores respectively. The sections: rapidly changing mood, dieting and bingeing and strange experiences that are surprisingly common were not used to create scores as these symptoms do not fit neatly into an internalising/externalising dichotomy. All of these questions can be found in Supplementary Table 1.

Longitudinal Analysis

The msCCA-regression analysis described above was used to find relations between psychiatric symptoms and neuroimaging measures of brain structure at age 19, when participants were young adults. However, the developmental time period immediately preceding this time point is also of potential interest, with the brain going through important maturational processes and participants being at increased risk for the development of psychopathology[76]. Thus, we applied the msCCA-regression algorithm between psychiatric symptoms and neuroimaging measures at age 14. The results of this analysis are show in Supplementary Figure 8. We did not find a significant relation between psychiatric symptoms and the brain at this age. As rs-fMRI data is only available for a small sub-sample of the full dataset at age 14, we only used VBM and TBSS data in this analysis.

It is possible that neuroimaging markers of psychiatric illness precede the development of full-blown psychiatric symptomatology. To determine whether this was the case in the present investigation, we took the TBSS and VBM regions identified as being associated with psychopathology at age 19, we then extracted the appropriate neuroimaging data from these brain regions at age 14, and correlated the output with symptoms at age 19. In this way, we showed that neuroimaging measures at age 14 have predictive value for psychopathology at age 19.

For these analyses, we used the same subjects as were included in our analysis at age 19. We also used the same train-test split within this subject group. We subjected this age 14 data to the same QC procedures as the data taken at age 19. Of the n = 666 subjects used in the msCCA-regression analysis carried out at age 19, 72 subjects had data that did not pass QC at age 14. This left n = 594

subjects for age 14 analyses, with n = 412 subjects in the training group and n = 182 in the testing/replication group.

Clinical Analyses

Using mSCCA-regression, we found a set of neuroimaging features that correlate with a set of questions assessing psychiatric health. At the group level, participants who score more highly on the vector derived from neuroimaging data will suffer a larger number of psychiatric symptoms (as measured by the DAWBA). It might therefore be expected that participants with a clinical diagnosis of a psychiatric disorder would score more highly on this neuroimaging vector than healthy controls. To discover whether this was the case, we subjected clinical data to exactly the same pre-processing as the IMAGEN data; we then looked for changes in grey matter volume in the regions identified in the initial analysis. A (one-sided) two-sample t-test was used to determine whether patients and controls differed significantly on this one-dimensional measure. We only used grey matter data here as this data-type showed the strongest relation to psychopathology in the IMAGEN sample. Furthermore, this data-type is widely available and the number of degrees of freedom in the MRI scan acquisition parameters is low. The case-control tests we used here make the assumption of data normality, although this was not formally tested here.

We used the same confounds in this analysis as we did on the IMAGEN data, this includes the use of total grey matter as a covariate of no interest. However, it could still be argued that regional changes are only acting as a proxy for total grey matter. In order to determine whether this is the case, we repeated all pertinent analyses,

using total grey matter as a regressor in addition to total intracranial volume. The results of these analyses are shown in Supplementary Figure 10.

Depression sample

The Munich sample consisted of patients with first episode and recurrent unipolar Depression treated as in-patients at the Max Planck Institute of Psychiatry, Munich, and healthy control participants. The data for 13 of the participants assessed was not used as it was deemed to be of insufficient quality, this left: N=614; 400 patients, age 48 [SD 13.8] years, 53% women; 214 control participants age 49 [SD 13.3] years, 58% women, for the most part overlapping with imaging genetic and MDD association studies reported in collaboration with the ENIGMA consortium[22,77]. Other than in the two flagship studies, no bipolar patients were included for reasons of clinical homogeneity. MDD diagnoses were based on clinical consensus in addition to M-CIDI or SCAN interviews, depending on the original study protocols. The Munich sample comprised images acquired in subsamples of the Munich Antidepressant Response Signature Study and the Recurrent Unipolar Depression Case-Control study, both performed at the MPIP. We did not use any statistical analyses to decide on the sample size used here. However, the sample used was among the largest of any single study investigating alterations in brain structure in depressed participants[77].

Schizophrenia/Bipolar sample

Participants with schizophrenia and bipolar disorder were recruited from the Thematically Organised Psychosis (TOP) study. This is a collaborative study based at the University of Oslo in Norway. The data for 2 participants was not used as it

was considered to be of insufficient quality, this left: 286 Controls (aged 34 [SD 9.5] years, 46% women), 161 Schizophrenics (aged 32 [SD 8.8] years, 35% women) and 189 participants with Bipolar Disorder (aged 34 [SD 11.5] years, 58% women). Patients were recruited from the psychiatric unit of Oslo University Hospital and were assessed for psychiatric illness with the Structural Clinical Interview for DSM-IV Axis I disorders (SCID-I). This assessment was either administered by an MD, or a clinically trained psychologist, and was used to assess the presence of AXIS I disorders. Before participation, control participants were screened to exclude serious somatic and psychiatric illness, substance abuse, or MRI-incompatibility. All participants gave written informed consent before participation. Further information about this sample and the scan protocols used can be found in Rimol, L. M. et al[78]. We did not use any statistical methods to pre-define the sample size used in this investigation. Nevertheless, the sample used is among the largest of any investigating structural brain alterations in Schizophrenia[79] and Bipolar disorder[41]

ADHD sample

Data for the ADHD sample was taken from the NeuroIMAGE project, a clinical cohort study. The study is made up of individuals tested at two different sites in the Netherlands, The Donders Centre for Cognitive Neuroimaging in Nijmegen, and the Vrije Universiteit in Amsterdam. The total sample consisted of 184 participants suffering from ADHD, 103 unaffected siblings, and 128 healthy controls. Further information on the participants and the protocols used can be found in von Rhein et al[80]. This sample includes a number of very young participants, which is likely to introduce a large degree of heterogeneity into the analysis. For this reason, we did not analyse the data from participants under the age of fifteen. This age divide point

was considered to offer a reasonable trade-off between sample homogeneity and size. The data for 12 of the participants was not used as it was deemed to be of insufficient quality. Case-control Analyses were made between 74 healthy controls (aged 18 [SD 2.0] years, 50% women) and 131 ADHD participants (aged 18 [SD 2.3] years, 27% women). No formal statistical methods were used to determine the size of this sample. However, this sample is large compared to similar samples investigating case-control differences in brain structure in patients with ADHD[81].

Data Availability Statement

IMAGEN data used in this investigation will be made available upon reasonable request to the corresponding author. All other data is available upon reasonable request addressed to the appropriate study leads.

Code Availability Statement

The core code used to run the analyses reported in this study are available as Supplementary Software. Supporting code can be found at: https://github.com/alexjamesing/mscca-regression-code.

References

1. Kessler RC, Amminger GP, Aguilar-Gaxiola S, Alonso J, Lee S, Ustun TB. Age of onset of mental disorders: A review of recent literature. *Curr Opin Psychiatry*. 2007;20(4):359-364.

2. Giedd JN, Blumenthal J, Jeffries NO, et al. Brain development during childhood and adolescence: A longitudinal MRI study. *Nat Neurosci*. 1999;2(10):861-863.

3. Steinberg L. Risk taking in adolescence: New perspectives from brain and behavioral science. *Current directions in psychological science*. 2007;16(2):55-59.

4. Gogtay N, Giedd JN, Lusk L, et al. Dynamic mapping of human cortical development during childhood through early adulthood. *Proc Natl Acad Sci U S A*. 2004;101(21):8174-8179.

5. Drysdale AT, Grosenick L, Downar J, et al. Resting-state connectivity biomarkers define neurophysiological subtypes of depression. *Nat Med*. 2016.

6. Insel T, Cuthbert B, Garvey M, et al. No title. *Research domain criteria (RDoC): toward a new classification framework for research on mental disorders*. 2010.

7. Lahey BB, Applegate B, Hakes JK, Zald DH, Hariri AR, Rathouz PJ. Is there a general factor of prevalent psychopathology during adulthood? *J Abnorm Psychol*. 2012;121(4):971.

8. Zhang X, Mormino EC, Sun N, et al. Bayesian model reveals latent atrophy factors with dissociable cognitive trajectories in alzheimer's disease. *Proc Natl Acad Sci U S A*. 2016;113(42):E6544.

9. Rosenberg MD, Finn ES, Scheinost D, et al. A neuromarker of sustained attention from whole-brain functional connectivity. *Nat Neurosci*. 2016;19(1):165.

10. Smith SM, Nichols TE, Vidaurre D, et al. A positive-negative mode of population covariation links brain connectivity, demographics and behavior. *Nat Neurosci*. 2015;18(11):1565-1567.

11. Witten DM, Tibshirani R, Hastie T. A penalized matrix decomposition, with applications to sparse principal components and canonical correlation analysis. *Biostatistics*. 2009;10(3):515-534.

12. Xia CH, Ma Z, Ciric R, et al. Linked dimensions of psychopathology and connectivity in functional brain networks. *Nature communications*. 2018;9(1):3003.

14. Goodman R, Ford T, Richards H, Gatward R, Meltzer H. The development and well-being assessment: Description and initial validation of an integrated assessment of child and adolescent psychopathology. *Journal of child psychology and psychiatry*. 2000;41(05):645-655.

15. Ashburner J. A fast diffeomorphic image registration algorithm. *Neuroimage*. 2007;38(1):95-113.

16. Smith SM, Jenkinson M, Johansen-Berg H, et al. Tract-based spatial statistics: Voxelwise analysis of multi-subject diffusion data. *Neuroimage*. 2006;31(4):1487-1505.

17. Miller KL, Alfaro-Almagro F, Bangerter NK, et al. Multimodal population brain imaging in the UK biobank prospective epidemiological study. *Nat Neurosci*. 2016;19(11):1523.

18. Ashburner J, Friston KJ. Voxel-based morphometry—the methods. *Neuroimage*. 2000;11(6):805-821.

19. Smith SM, Jenkinson M, Johansen-Berg H, et al. Tract-based spatial statistics: Voxelwise analysis of multi-subject diffusion data. *Neuroimage*. 2006;31(4):1487-1505.

20. Power JD, Fair DA, Schlaggar BL, Petersen SE. The development of human functional brain networks. *Neuron*. 2010;67(5):735-748.

21. Meinshausen N, Bühlmann P. Stability selection. *Journal of the Royal Statistical Society: Series B (Statistical Methodology)*. 2010;72(4):417-473.

22. Schmaal L, Hibar DP, Sämann PG, et al. Cortical abnormalities in adults and adolescents with major depression based on brain scans from 20 cohorts worldwide in the ENIGMA major depressive disorder working group. *Mol Psychiatry*. 2016.

23. Chen G, Hu X, Li L, et al. Disorganization of white matter architecture in major depressive disorder: A meta-analysis of diffusion tensor imaging with tract-based spatial statistics. *Scientific reports*. 2016;6:21825.

24. Guo W, Liu F, Liu J, et al. Increased cerebellar-default-mode-network connectivity in drug-naive major depressive disorder at rest. *Medicine*. 2015;94(9).

25. Carmona S, Vilarroya O, Bielsa A, et al. Global and regional gray matter reductions in ADHD: A voxel-based morphometric study. *Neurosci Lett*. 2005;389(2):88-93.

26. Krueger RF, Caspi A, Moffitt TE, Silva PA. The structure and stability of common mental disorders (DSM-III-R): A longitudinal-epidemiological study. *J Abnorm Psychol*. 1998;107(2):216.

27. Diedenhofen B, Musch J. Cocor: A comprehensive solution for the statistical comparison of correlations. *PloS one*. 2015;10(4):e0121945.

28. Dunn OJ, Clark V. Correlation coefficients measured on the same individuals. *Journal of the American Statistical Association*. 1969;64(325):366-377.

29. Whelan R, Watts R, Orr CA, et al. Neuropsychosocial profiles of current and future adolescent alcohol misusers. *Nature*. 2014;512(7513):185-189.

30. Lahey BB, Van Hulle CA, Singh AL, Waldman ID, Rathouz PJ. Higher-order genetic and environmental structure of prevalent forms of child and adolescent psychopathology. *Arch Gen Psychiatry*. 2011;68(2):181-189.

31. Kessler RC, Angermeyer M, Anthony JC, et al. Lifetime prevalence and age-of-onset distributions of mental disorders in the world health organization's world mental health survey initiative. *World Psychiatry*. 2007;6(3):168-176.

32. Mayberg HS. Modulating dysfunctional limbic-cortical circuits in depression: Towards development of brain-based algorithms for diagnosis and optimised treatment. *Br Med Bull*. 2003;65(1):193-207.

33. Witelson SF. Hand and sex differences in the isthmus and genu of the human corpus callosum: A postmortem morphological study. *Brain*. 1989;112(3):799-835.

34. Tham MW, San Woon P, Sum MY, Lee T, Sim K. White matter abnormalities in major depression: Evidence from post-mortem, neuroimaging and genetic studies. *J Affect Disord*. 2011;132(1-2):26-36.

35. Chen G, Hu X, Li L, et al. Disorganization of white matter architecture in major depressive disorder: A meta-analysis of diffusion tensor imaging with tract-based spatial statistics. *Scientific reports*. 2016;6:21825.

36. Raichle ME, MacLeod AM, Snyder AZ, Powers WJ, Gusnard DA, Shulman GL. A default mode of brain function. *Proceedings of the National Academy of Sciences*. 2001;98(2):676-682.

37. Buckner RL, Andrews-Hanna JR, Schacter DL. The brain's default network. *Ann N Y Acad Sci*. 2008;1124(1):1-38.

1203 38. Ray RD, Ochsner KN, Cooper JC, Robertson ER, Gabrieli JD, Gross JJ. Individual differences in trait
1204 rumination and the neural systems supporting cognitive reappraisal. *Cognitive, Affective, &*
1205 *Behavioral Neuroscience*. 2005;5(2):156-168.

1206 39. Stoodley CJ. The cerebellum and cognition: Evidence from functional imaging studies. *The*
1207 *Cerebellum*. 2012;11(2):352-365.

1208 40. Guggenmos M, Schmack K, Sekutowicz M, et al. Quantitative neurobiological evidence for
1209 accelerated brain aging in alcohol dependence. *Translational psychiatry*. 2017;7(12):1279.

1210 41. Hibar DP, Westlye LT, Doan NT, et al. Cortical abnormalities in bipolar disorder: An MRI analysis
1211 of 6503 individuals from the ENIGMA bipolar disorder working group. *Mol Psychiatry*. 2017.

1212 42. McGorry PD, Hickie IB, Yung AR, Pantelis C, Jackson HJ. Clinical staging of psychiatric disorders: A
1213 heuristic framework for choosing earlier, safer and more effective interventions. *Aust N Z J*
1214 *Psychiatry*. 2006;40(8):616-622.

1215 43. Biswal B, Zerrin Yetkin F, Haughton VM, Hyde JS. Functional connectivity in the motor cortex of
1216 resting human brain using echo-planar MRI. *Magnetic resonance in medicine*. 1995;34(4):537-541.

1217 44. Schumann G, Loth E, Banaschewski T, et al. The IMAGEN study: Reinforcement-related behaviour
1218 in normal brain function and psychopathology. *Mol Psychiatry*. 2010;15(12):1128-1139.

1219 45. Goodman R. The strengths and difficulties questionnaire: A research note. *Journal of child*
1220 *psychology and psychiatry*. 1997;38(5):581-586.

1221 46. Vulser H, Lemaitre H, Artiges E, et al. Subthreshold depression and regional brain volumes in
1222 young community adolescents. *Journal of the American Academy of Child & Adolescent Psychiatry*.
1223 2015;54(10):832-840.

1224 47. Ashburner J, Friston KJ. Unified segmentation. *Neuroimage*. 2005;26(3):839-851.

48. Grellmann C, Bitzer S, Neumann J, et al. Comparison of variants of canonical correlation analysis and partial least squares for combined analysis of MRI and genetic data. *Neuroimage*. 2015;107:289-310.

49. Jones DK, Williams SCR, Gasston D, Horsfield MA, Simmons A, Howard R. Isotropic resolution diffusion tensor imaging with whole brain acquisition in a clinically acceptable time. *Hum Brain Mapp*. 2002;15(4):216-230.

50. Smith SM, Jenkinson M, Woolrich MW, et al. Advances in functional and structural MR image analysis and implementation as FSL. *Neuroimage*. 2004;23:S219.

51. Avants BB, Tustison NJ, Song G, Cook PA, Klein A, Gee JC. A reproducible evaluation of ANTs similarity metric performance in brain image registration. *Neuroimage*. 2011;54(3):2033-2044.

52. Pruim RH, Mennes M, van Rooij D, Llera A, Buitelaar JK, Beckmann CF. ICA-AROMA: A robust ICA-based strategy for removing motion artifacts from fMRI data. *Neuroimage*. 2015;112:267-277.

53. Pruim RH, Mennes M, Buitelaar JK, Beckmann CF. Evaluation of ICA-AROMA and alternative strategies for motion artifact removal in resting state fMRI. *Neuroimage*. 2015;112:278-287.

54. Behzadi Y, Restom K, Liau J, Liu TT. A component based noise correction method (CompCor) for BOLD and perfusion based fMRI. *Neuroimage*. 2007;37(1):90-101.

55. Fischl B. FreeSurfer. *Neuroimage*. 2012;62(2):774-781.

56. Power JD, Cohen AL, Nelson SM, et al. Functional network organization of the human brain. *Neuron*. 2011;72(4):665-678.

57. Hotelling H. Relations between two sets of variates. *Biometrika*. 1936:321-377.

58. Witten DM, Tibshirani RJ. Extensions of sparse canonical correlation analysis with applications to genomic data. *Statistical applications in genetics and molecular biology*. 2009;8(1):1-27.

59. Parkhomenko E, Tritchler D, Beyene J. Sparse canonical correlation analysis with application to genomic data integration. *Statistical Applications in Genetics and Molecular Biology*. 2009;8(1):1-34.

60. Gifi A. *Nonlinear multivariate analysis.* John Wiley & Sons Incorporated; 1990.

61. Jenkins LM, Barba A, Campbell M, et al. Shared white matter alterations across emotional disorders: A voxel-based meta-analysis of fractional anisotropy. *NeuroImage: Clinical*. 2016;12:1022-1034.

62. Goodkind M, Eickhoff SB, Oathes DJ, et al. Identification of a common neurobiological substrate for mental illness. *JAMA psychiatry*. 2015;72(4):305-315.

63. Everitt BS, Dunn G. *Applied multivariate data analysis.* Vol 2. Arnold London; 2001.

64. Timm NH, Carlson JE. Part and bipartial canonical correlation analysis. *Psychometrika*. 1976;41(2):159-176.

65. O'Brien LM, Ziegler DA, Deutsch CK, Frazier JA, Herbert MR, Locascio JJ. Statistical adjustments for brain size in volumetric neuroimaging studies: Some practical implications in methods. *Psychiatry Research: Neuroimaging*. 2011;193(2):113-122.

66. Pell GS, Briellmann RS, Chan CHP, Pardoe H, Abbott DF, Jackson GD. Selection of the control group for VBM analysis: Influence of covariates, matching and sample size. *Neuroimage*. 2008;41(4):1324-1335.

67. Voevodskaya O, Simmons A, Nordenskjöld R, et al. The effects of intracranial volume adjustment approaches on multiple regional MRI volumes in healthy aging and alzheimer's disease. *Frontiers in aging neuroscience*. 2014;6.

68. Van Den Wollenberg, Arnold L. Redundancy analysis an alternative for canonical correlation analysis. *Psychometrika*. 1977;42(2):207-219.

69. Stewart D, Love W. A general canonical correlation index. *Psychol Bull*. 1968;70(3):160-163.

70. Monteiro JM, Rao A, Shawe-Taylor J, Mourão-Miranda J, Alzheimer's Disease Initiative. A multiple hold-out framework for sparse partial least squares. *J Neurosci Methods*. 2016;271:182-194.

71. Holmes AP, Blair RC, Watson G, Ford I. Nonparametric analysis of statistic images from functional mapping experiments. *Journal of Cerebral Blood Flow & Metabolism*. 1996;16(1):7-22.

72. Westfall PH, Troendle JF. Multiple testing with minimal assumptions. *Biometrical Journal*. 2008;50(5):745-755.

73. Westfall PH, Young SS. *Resampling-based multiple testing: Examples and methods for p-value adjustment.* Vol 279. John Wiley & Sons; 1993.

74. Friedman J, Hastie T, Tibshirani R. *The elements of statistical learning.* Vol 1. Springer series in statistics New York; 2001.

75. Aebi M, Kuhn C, Metzke CW, Stringaris A, Goodman R, Steinhausen H. The use of the development and well-being assessment (DAWBA) in clinical practice: A randomized trial. *Eur Child Adolesc Psychiatry*. 2012;21(10):559-567.

76. Steinberg L. Cognitive and affective development in adolescence. *Trends Cogn Sci (Regul Ed)*. 2005;9(2):69-74.

77. Schmaal L, Veltman DJ, van Erp TG, et al. Subcortical brain alterations in major depressive disorder: Findings from the ENIGMA major depressive disorder working group. *Mol Psychiatry*. 2016;21(6):806.

78. Rimol LM, Nesvåg R, Hagler DJ, et al. Cortical volume, surface area, and thickness in schizophrenia and bipolar disorder. *Biol Psychiatry*. 2012;71(6):552-560.

79. van Erp TG, Hibar DP, Rasmussen JM, et al. Subcortical brain volume abnormalities in 2028 individuals with schizophrenia and 2540 healthy controls via the ENIGMA consortium. *Mol Psychiatry*. 2016;21(4):547.

80. von Rhein D, Mennes M, van Ewijk H, et al. The NeuroIMAGE study: A prospective phenotypic, cognitive, genetic and MRI study in children with attention-deficit/hyperactivity disorder. design and descriptives. *Eur Child Adolesc Psychiatry*. 2015;24(3):265-281.

81. Hoogman M, Bralten J, Hibar DP, et al. Subcortical brain volume differences in participants with attention deficit hyperactivity disorder in children and adults: A cross-sectional mega-analysis. *The Lancet Psychiatry*. 2017;4(4):310-319.

Acknowledgments

This work received support from the following sources: the European Union-funded FP6 Integrated Project IMAGEN (Reinforcement-related behaviour in normal brain function and psychopathology) (LSHM-CT- 2007-037286), the Horizon 2020 funded ERC Advanced Grant 'STRATIFY' (Brain network based stratification of reinforcement-related disorders) (695313), ERANID (Understanding the Interplay between Cultural, Biological and Subjective Factors in Drug Use Pathways) (PR-ST-0416-10004), BRIDGET (JPND: BRain Imaging, cognition Dementia and next generation GEnomics) (MR/N027558/1), Human Brain Project (HBP SGA 2, 785907), the FP7 project MATRICS (603016), the Medical Research Council Grant 'c-VEDA' (Consortium on Vulnerability to Externalizing Disorders and Addictions) (MR/N000390/1), the National Institute for Health Research (NIHR) Biomedical Research Centre at South London and Maudsley NHS Foundation Trust and King's College London, the Bundesministeriumfür Bildung und Forschung (BMBF grants 01GS08152; 01EV0711; Forschungsnetz AERIAL 01EE1406A, 01EE1406B , 01ZX1314G, 01GS08147), the Deutsche Forschungsgemeinschaft (DFG grants SM 80/7-2, SFB 940/2), the Medical Research Foundation and Medical Research Council (grants MR/R00465X/1 and MR/S020306/1), the National Institutes of Health (NIH) funded ENIGMA (grants 5U54EB020403-05 and 1R56AG058854-01). Further support was provided by grants from: ANR (project AF12-NEUR0008-01 - WM2NA, and ANR-12-SAMA-0004), the Fondation de France, the Fondation pour la Recherche Médicale, the Mission Interministérielle de Lutte-contre-les-Drogues-et-les-Conduites-Addictives (MILDECA), the Assistance-Publique-Hôpitaux-de-Paris and INSERM (interface grant), Paris Sud University IDEX 2012; the National Institutes of Health, Science Foundation Ireland (16/ERCD/3797), U.S.A. (Axon, Testosterone and Mental Health during Adolescence; RO1 MH085772-01A1), and by NIH Consortium grant U54 EB020403, supported by a

cross-NIH alliance that funds Big Data to Knowledge Centres of Excellence. AFM gratefully acknowledges funding from the Netherlands Organisation for Scientific Research via the Vernieuwingsimpuls VIDI programme (grant number 016.156.415). The funders had no role in study design, data collection and analysis, decision to publish, or preparation of the manuscript

Author Contributions

Author Contributions

Pre-processed data: AI, CC, IMV, PGS, HL, TJ, GR; **Analysed the data:** AI, PGS; **Wrote the manuscript:** AI, GS, FB, PGS**; Conceptualised the study:** AI, GS, TWR, AM, JA, EB**; Collected Data:** NT, EBQ, TW, SD, TB, ALWB, UB, CB, PC, TF, HF, VF, HG, PS, PG, YG, AH, BI, VK, JLM, AML, SB, FN, BVN, DPO, MLPM, SM, JP, LP, MS, AS, MNS, HW, RW, OAA, IA, EDB, JB; **Prepared Figures:** AI, NT **Revised Manuscript:** All Authors

Competing Interests

Dr. Banaschewski served in an advisory or consultancy role for Lundbeck, Medice, Neurim Pharmaceuticals, Oberberg GmbH, Shire. He received conference support or speaker's fee by Lilly, Medice, Novartis and Shire. He has been involved in clinical trials conducted by Shire & Viforpharma. He received royalities from Hogrefe, Kohlhammer, CIP Medien, Oxford University Press. The present work is unrelated to the above grants and relationships. Dr. Barker has received honoraria from General Electric Healthcare for teaching on scanner programming courses and acts as a consultant for IXICO. Dr. Andreassen received speaker's honorarium from Lundbeck. Gabriel Robert received financial support from scientific meetings (Janssen & Janssen, Otsuka-Lundbeck). Dr. Meyer-Lindenberg has received consultant fees from Boehringer Ingelheim, Brainsway, Elsevier, Lundbeck Int. Neuroscience Foundation and Science Advances. The other authors report no biomedical financial interests or potential conflicts of interest.

Figure 1: Results of the first msCCA-regression analysis showing relations between anxiety/depression psychiatric symptoms and neuroimaging measures in the IMAGEN sample. (a): The full msCCA-regression model linking psychiatric symptoms to VBM, TBSS and rs-fcMRI neuroimaging measures at age 19. We found associations between psychiatric symptoms and neuroimaging measures of r = 0.59(465) (p = < 0.001) in the training set, and associations between symptoms and the brain of r=0.23(197), p<0.001, 95% CIs=0.13, ∞ *in the test set; (b): Shows the msCCA-regression model linking psychiatric symptoms with the different neuroimaging measures (c): Psychiatric symptoms contributing to this relation are shown on the left, their canonical weights are shown in red. (d): rs-fcMRI measures of functional connectivity. (e): VBM measures of grey matter volume associated with symptoms. (f): TBSS measures of fractional anisotropy (FA).*

Figure 2: Results of the second msCCA-regression analyses showing relations between executive dysfunction symptoms and neuroimaging measures in the IMAGEN sample, following the removal of the first canonical relation. (a): The full msCCA-regression model linking psychiatric symptoms to VBM, TBSS and rs-fcMRI neuroimaging measures at age 19. We found associations between executive dysfunction symptoms and neuroimaging measures of r = 0.46 (p = 0.004) in the training set, and associations between symptoms and the brain of r = 0.19(197), p = 0.002, 95% CIs =0.087, ∞ *in the test set; (b) msCCA-regression model linking psychiatric symptoms with the different neuroimaging measures (c) Symptoms contributing to this relation are shown on the left their canonical weights are shown in red. (d) rs-fcMRI measures of functional connectivity. (e) VBM*

measures of grey matter volume associated with symptoms. (f): TBSS measures of fractional anisotropy (FA).

Figure 3: Longitudinal analysis of canonical correlates. (a) anxiety/depression symptom correlates: VBM and TBSS brain correlates established at age 19 are associated with anxiety/depression behavioural symptoms at age 19 (r =0.19(180), p = 0.003, 95% CIs=0.069,∞), but not at age 14 (r=0.020(180), p=0.40, 95% CIs=-0.10,∞). Brain correlates at 14 years predict the manifestation of behavioral symptoms at 19 years (r=0.14(180), p=0.023, 95% CIs=0.022,∞). (b) Executive dysfunction symptom correlates: VBM and TBSS correlates established at age 19 are associated with behavioral symptoms at age 19 (r =0.15(180), p = 0.024, 95% CIs=0.028,∞), but not at age 14 (r=0.030(180), p=0.41, 95% CIs=-0.093,∞). Brain correlates at 14 years do not predict the manifestation of behavioral symptoms at 19 years (r=0.11(180), p=0.065, 95% CIs =-0.010,∞).

Figure 4: Differences in the grey matter correlates of anxiety/depression and executive dysfunction psychiatric symptoms, between cases and controls for a range of psychiatric illnesses. For the box and whisker plots, the central mark in each box represents the median, with the top and bottom edges of the box indicating the 25th and 75th percentiles of the sample respectively, whiskers represent 1.5x the interquartile range and the hollow circles represent sample outliers. For display purposes, total grey matter in each case-control comparison is divided by the pooled standard deviation. The effect sizes (calculated using Cohen's D) relating to these differences are shown in the right-hand panel. (a): Differences in grey matter volume between patients and controls in the anxiety/depression set of grey matter correlates are shown in the left-hand panel. Clinical psychiatric disorders exhibited the following case-control differences: Depression: t-statistic=4.61(612), p<0.001, Cohen's D = 0.39, 95% CIs=0.25, ∞; Schizophrenia: t-statistic=2.54(445), p=0.002, Cohen's D=0.25, 95% CIs = 0.087, ∞; ADHD (t-statistic=1.84(203), p=0.034, Cohen's D=0.26, 95% CIs=0.030, ∞; Bipolar: (t-statistic=-0.23(473), p=0.59, Cohen's D=-0.02, 95% CIs=-0.17, ∞). (b): Differences in grey matter volume between patients and controls in the executive dysfunction set of grey matter correlates. Clinical psychiatric disorders exhibited the following case-control differences: Depression: t-statistic=1.65(612), p=0.050, Cohen's D=0.14, 95% CIs=0.001, ∞, Schizophrenia: t-statistic=2.81(445), p=0.0026, Cohen's D=0.28, 95% CIs=0.11, ∞; ADHD: t-statistic=2.19(203), p=0.014, Cohen's D=0.32, 95% CIs=0.070, ∞; Bipolar: t-statistic=-1.33(473), p=0.90, Cohen's D=-0.12, 95% CIs=-0.27, ∞.

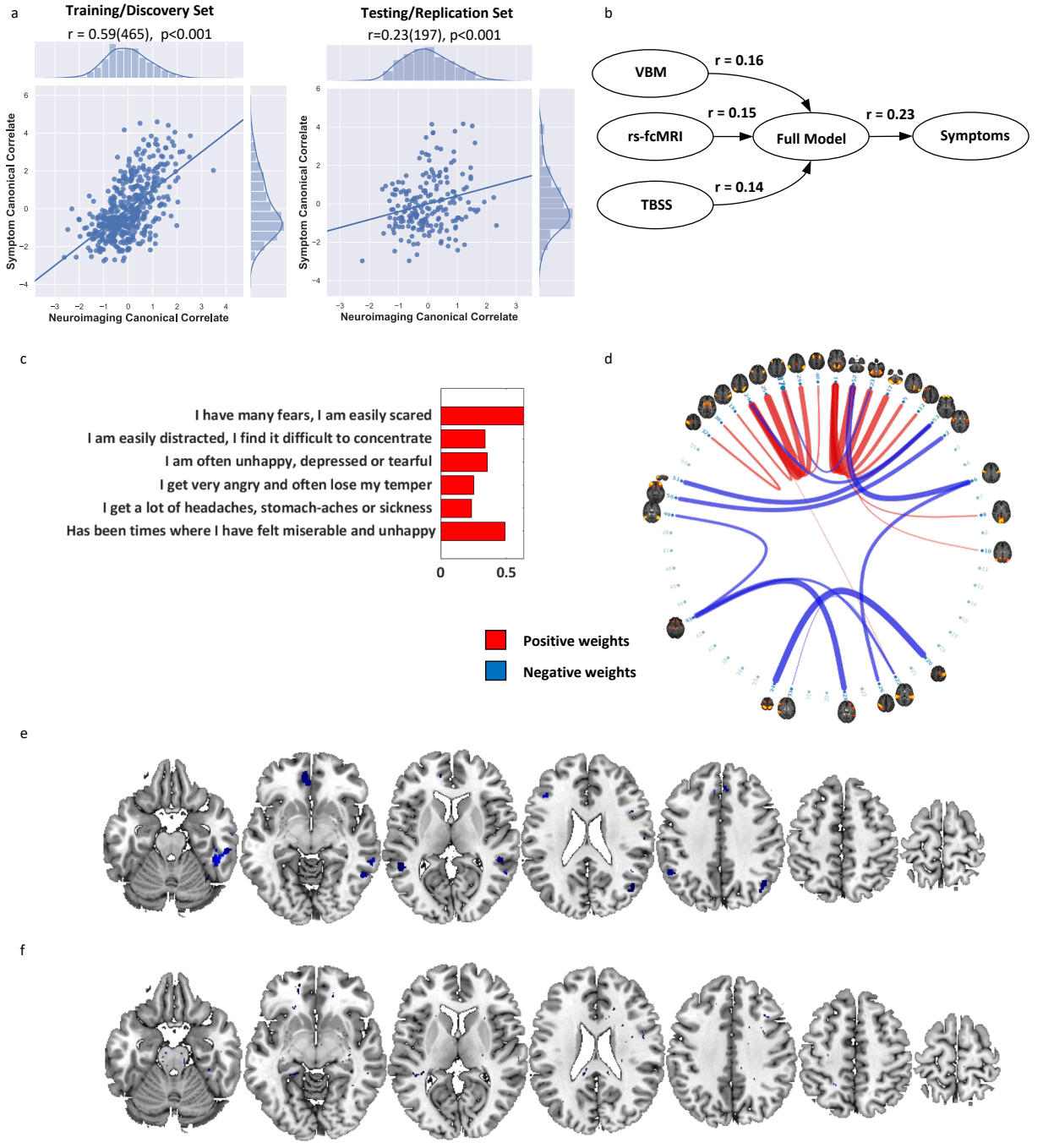
a
Training/Discovery Set
r = 0.59(465), p<0.001
Testing/Replication Set
r=0.23(197), p<0.001
Symptom Canonical Correlate
Neuroimaging Canonical Correlate
b
VBM
rs-fcMRI
TBSS
Full Model
Symptoms
r = 0.16
r = 0.15
r = 0.14
r = 0.23
c
I have many fears, I am easily scared
I am easily distracted, I find it difficult to concentrate
I am often unhappy, depressed or tearful
I get very angry and often lose my temper
I get a lot of headaches, stomach-aches or sickness
Has been times where I have felt miserable and unhappy
0
0.5
d
Positive weights
Negative weights
e
f

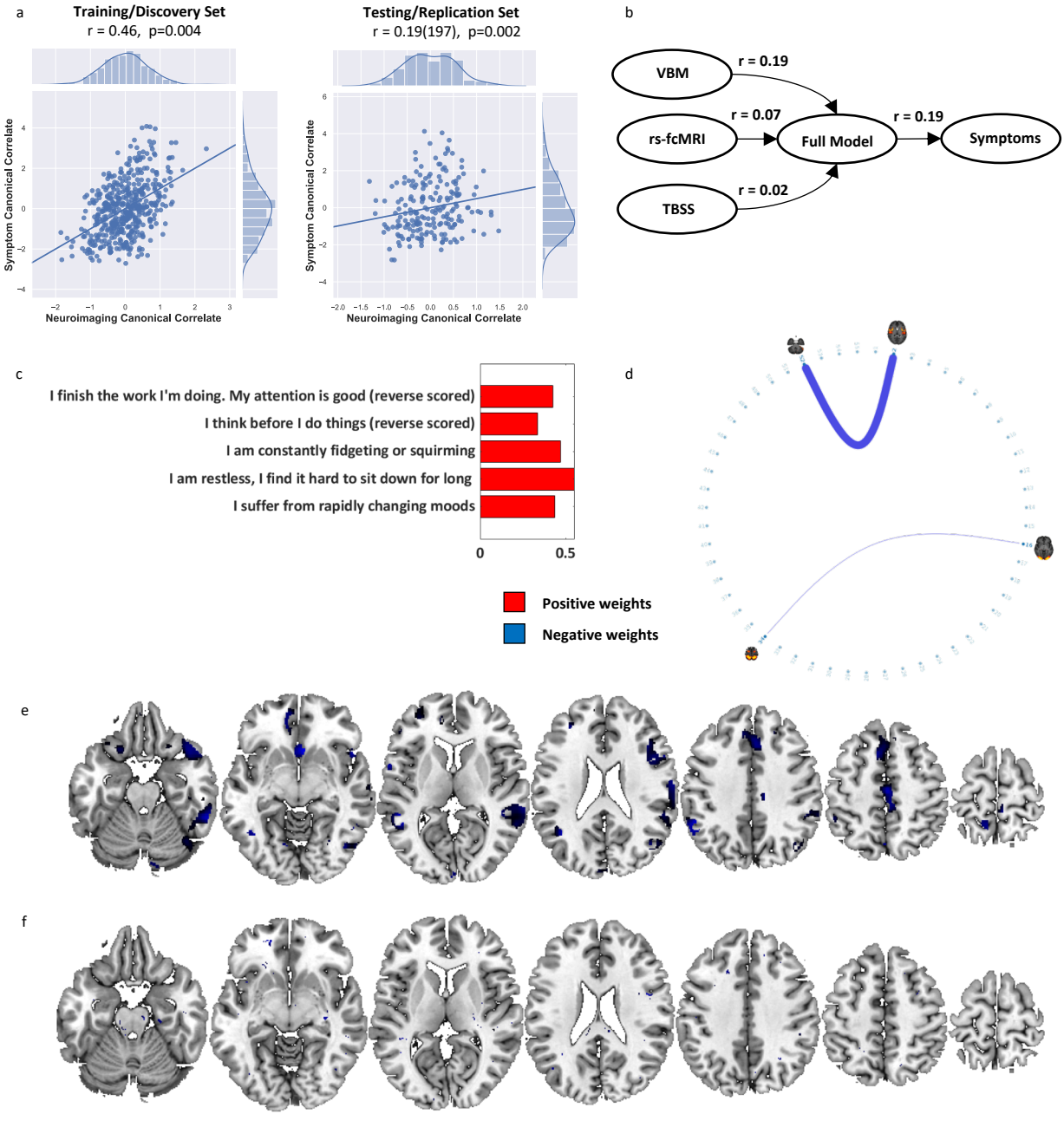
a
Training/Discovery Set
r = 0.46, p=0.004
Testing/Replication Set
r = 0.19(197), p=0.002
Symptom Canonical Correlate
Neuroimaging Canonical Correlate
b
VBM
rs-fcMRI
TBSS
Full Model
Symptoms
r = 0.19
r = 0.07
r = 0.19
r = 0.02
c
I finish the work I'm doing. My attention is good (reverse scored)
I think before I do things (reverse scored)
I am constantly fidgeting or squirming
I am restless, I find it hard to sit down for long
I suffer from rapidly changing moods
0
0.5
Positive weights
Negative weights
d
e
f

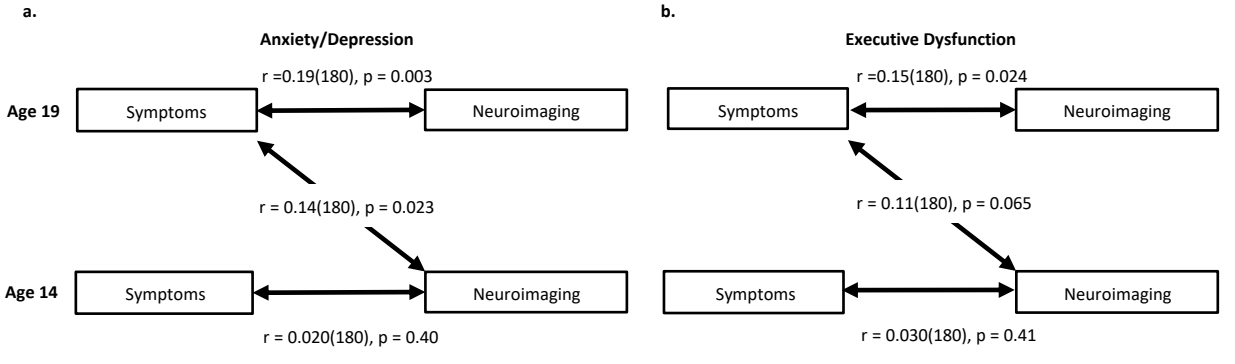
a.
Anxiety/Depression
r =0.19(180), p = 0.003
Age 19
Symptoms
Neuroimaging
r = 0.14(180), p = 0.023
Age 14
Symptoms
Neuroimaging
r = 0.020(180), p = 0.40
b.
Executive Dysfunction
r =0.15(180), p = 0.024
Symptoms
Neuroimaging
r = 0.11(180), p = 0.065
Symptoms
Neuroimaging
r = 0.030(180), p = 0.41

a.

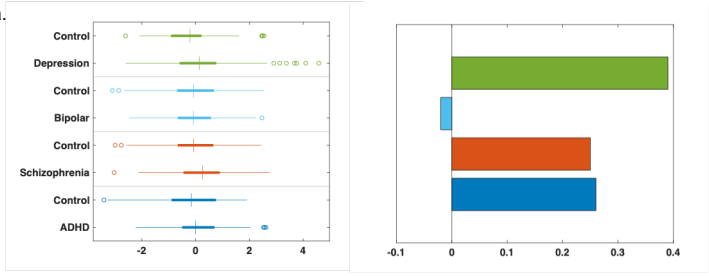

t-statistic=4.61(612), p<0.001, Cohen's D = 0.39

t-statistic=-0.23(473), p=0.59, Cohen's D=-0.02

t-statistic=2.54(445), p=0.002, Cohen's D=0.25

t-statistic=1.84(203), p=0.034, Cohen's D=0.26

b.

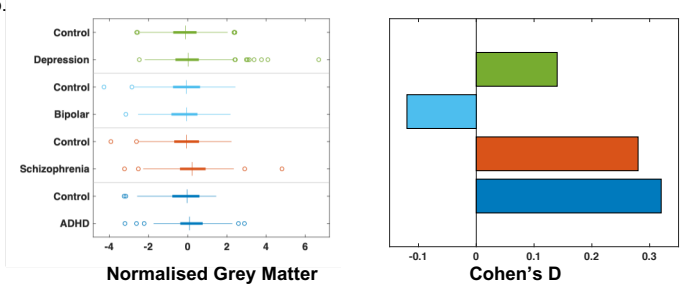

t-statistic=1.65(612), p=0.050, Cohen's D=0.14

t-statistic=-1.33(473), p=0.90, Cohen's D=-0.12

t-statistic=2.81(445), p=0.0026, Cohen's D=0.28

t-statistic=2.19(203), p=0.014, Cohen's D=0.32